

Color characteristics of the fringe-field switching liquid crystal mode depending on E- and O-modes

H.Y. Kim ^{a,b}, I.S. Song ^a, I.-S. Baik ^a, S.Y. Kim ^b, S.H. Lee ^{a,*}

^a School of Advanced Materials Engineering, Chonbuk National University, Chonju, Chonbuk 561-756, Republic of Korea

^b SBU Development Center, BOE_TFT_LCD_SBU, San 136-1, Ami-ri, Bubal-eup, Ichon, Kyungki-do 467-701, Republic of Korea

Received 11 August 2005; accepted 27 February 2006

Available online 30 June 2006

Abstract

Color characteristics of the E- and O-modes in the fringe-field switching mode using the liquid crystal with negative dielectric anisotropy have been investigated. According to calculated and measured results for color shift up to 70° of polar angle in all directions, a cell with E-mode shows smaller color shift with varying viewing direction than a cell with O-mode in all grey levels, for instance, the color shift in a white state is much smaller in the E-mode ($\Delta xy = 0.1819$) than in the O-mode ($\Delta xy = 0.0798$). However, the color shift of the white state is strongly suppressed for both E-mode ($\Delta xy = 0.0199$) and O-mode ($\Delta xy = 0.0093$) with a dual domain structure.

© 2006 Elsevier B.V. All rights reserved.

PACS: 85.60.-q; 85.60.Bt

Keywords: Fringe-field switching mode; E- and O-mode; Color characteristics

1. Introduction

Recently, the replacement of the cathode ray tube by liquid crystal displays (LCDs) in many application fields has become a general tendency because the image quality of the LCDs has been greatly improved owing to extensive research on many new modes. Three of the major LC modes are in-plane switching (IPS) mode [1], fringe-field switching (FFS) mode [2–6], and multi-domain vertical alignment (MVA) mode [7]. Especially, the IPS and FFS modes show wide viewing angle due to in-plane rotation of the LC director, but they have a disadvantage at a dark state in that light leakage occurs in oblique viewing directions. In order to solve such a problem, a compensation film has been employed, in which the O-mode is more effective to reduce the light leakage than the E-mode [8,9]. Also, both LC modes show better process margin with the O-mode than the E-mode in terms of the contrast ratio (CR) [10].

To achieve a good dark state with compensated film and a high CR in the FFS mode, the O-mode has an advantage. Nevertheless, color purity at oblique viewing directions as well as at normal directions is also an important factor in LCDs. Therefore, we have studied the electro-optic and color characteristics of the E- and O-modes in the FFS mode using a liquid crystal with negative dielectric anisotropy.

2. Cell structure and switching principle of FFS mode

Fig. 1 describes a schematic cross sectional view of the FFS mode with a local director orientation in both off- and on-states. In the FFS mode, the electrodes exist only at the bottom substrate. In general, common electrodes exist as planes and pixel electrodes exist in slit form with suitable gaps (l) between them. With this electrode structure, a fringe-electric field is generated when voltage is applied and, more importantly, a strong horizontal field exists near the bottom surface at the edge of each pixel electrode [11].

The normalized light transmission of a device with a uniaxial LC medium under a crossed polarizer is given by

* Corresponding author. Tel.: +82 63 270 2343; fax: +82 63 270 2341.
E-mail address: lsh1@chonbuk.ac.kr (S.H. Lee).

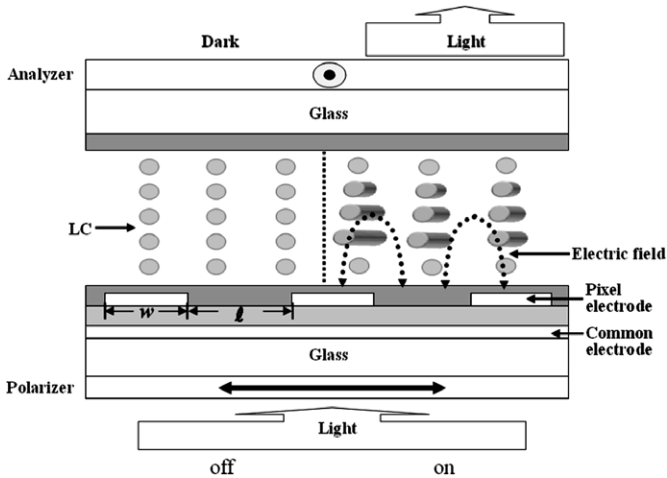


Fig. 1. Schematic cross-sectional view of on- and off-state in a FFS mode.

$$T/T_0 = \sin^2(2\psi(V)) \sin^2(\pi d \Delta n_{\text{eff}}(\theta, \Phi, \lambda)/\lambda), \quad (1)$$

where ψ is a voltage-dependent angle between the transmission axes of the crossed polarizers and the LC director, d is a cell gap, Δn_{eff} is an effective birefringence of the LC layer dependent on polar (θ) and azimuthal (Φ) angle in spherical coordinates, and λ is the wavelength of the incident light. In the FFS mode, the LCs are homogeneously aligned at an initial state and, before applying voltage, the optical axis of LC molecules coincides with the polarizer ($\psi = 0^\circ$), so that the polarization state of incident light through the LC layer is not changed. Therefore, the transmitted light is blocked by analyzers in the off-state. With bias voltage, the optical axis of LC molecules deviates from the transmission axis of the polarizer by fringe field, so that the polarization state of incident light changes before facing the analyzer. Thus, light can be transmitted. In a white state of the IPS mode using transparent electrodes, two different degrees of the LC rotations can be considered at two positions, between electrodes and above electrodes, such that the twisted angle is much higher between electrodes than above electrodes. However, in the FFS mode, the intensity of the horizontal field to rotate the LC is alternating along electrodes periodically, so that the rotation degree of the LC director oscillates, resulting in the highest twist angle near the bottom surface at the edge of electrodes and below the LC middle layer at the center of electrodes, as shown in Fig. 1 [12]. Therefore, the effective retardation of the LC cell could be different in viewing directions depending on the O- and E-modes defined at where the transmission axis of the bottom polarizer orients parallel (E-mode) or perpendicular (O-mode) to the LC director.

3. Electro-optic and color characteristics with O- and E-mode

First of all, to analyze electro-optic and color characteristics in the FFS mode, calculations are performed by using

the LCD master (Shintech, Japan). Here, the width of the pixel electrode (w) and the gap are assumed to be 3 and 4.5 μm , respectively. The passivation layer, with thickness of 3000 \AA , is positioned between the pixel and the common electrodes. A LC with physical parameters such as dielectric anisotropy $\Delta\epsilon = -4.0$, $\Delta n = 0.9$ at 550 nm, and elastic constants $K_1 = 13.5 \text{ pN}$, $K_2 = 6.5 \text{ pN}$, $K_3 = 15.1 \text{ pN}$ is used. The surface tilt angle of the LC is 2° with initial rubbing direction of 12° anticlockwise with respect to the horizontal component of a fringe-electric field, and a cell gap is 4 μm . To calculate the transmittance, a 2×2 extended Jones matrix has been used [13]. In addition, the transmittance of a single polarizer was assumed to be 41% and the absorption through glass and electrode was neglected.

Fig. 2 shows the calculated voltage-dependent transmittance (normalized transmission) (V - T) curves of the device with the O- and E-modes at a normal direction. The V - T curves with the O- and E-modes coincide with each other, indicating that the effective cell retardations as a function of applied voltage are the same as each other. Next, viewing angle characteristics in terms of luminance uniformity and iso-contrast ratio (CR) curve with the O- and E-modes are calculated. Two grey levels, such as mid-grey (T_{50}) and full white state (T_{100}) are compared, as shown in Fig. 3. In comparison of mid-grey, the iso-luminance curves representing relative transmittance of 30% (R_{30}), 50% (R_{50}), and 70% (R_{70}) with respect to the maximal transmittance at a normal direction do not coincide with each other, such that the shape of R_{50} and R_{30} is closer to that of an ellipse in the E-mode than in the O-mode. This ellipse-like shape indicates that the change in ratio of luminance along azimuthal directions at a specific polar angle is larger than that for a circular shape. The luminance uniformity in white state is slightly better in the E-mode than in the O-mode such that the iso-luminance curve for R_{30} does not exist in the E-mode within 80° of a polar angle in all azimuthal directions, and R_{70} and R_{50} have a circular shape. Nevertheless, the iso-contrast curve shows almost the same

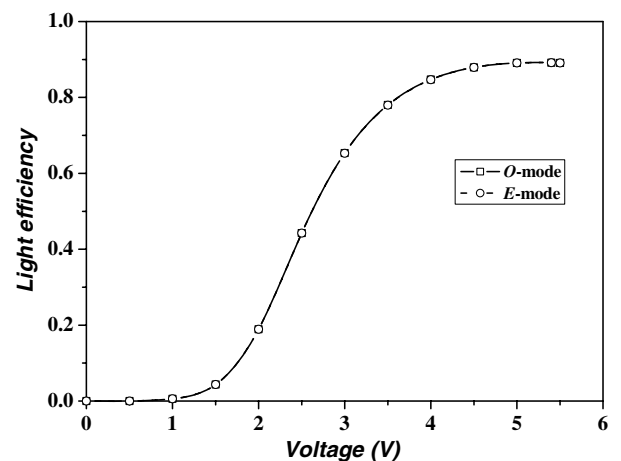


Fig. 2. Calculated voltage-dependent transmittance curves with O- and E-modes.

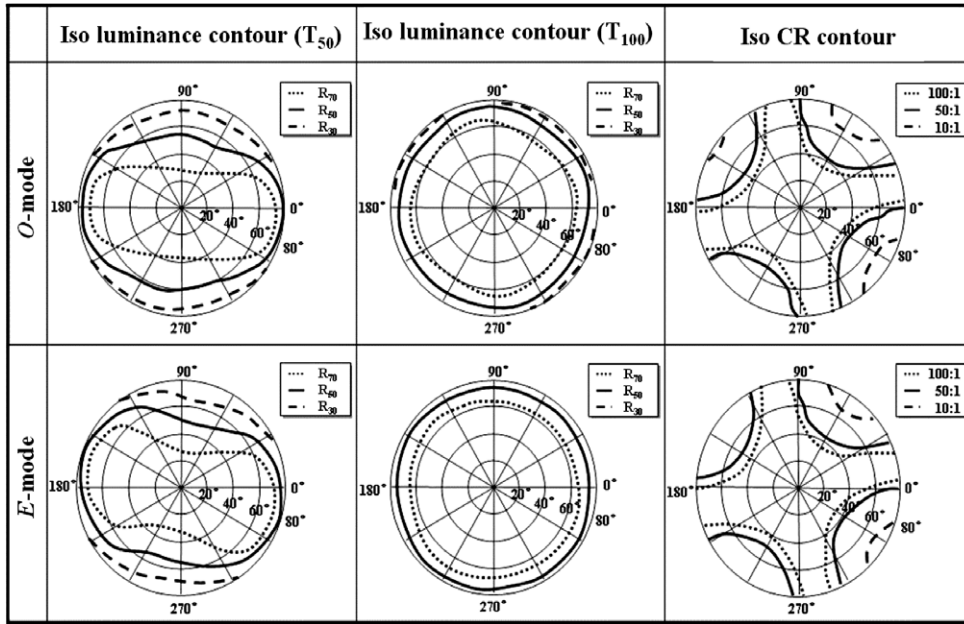


Fig. 3. Calculated iso-luminance and iso-contrast ratio contours of the FFS mode with O- and E-modes.

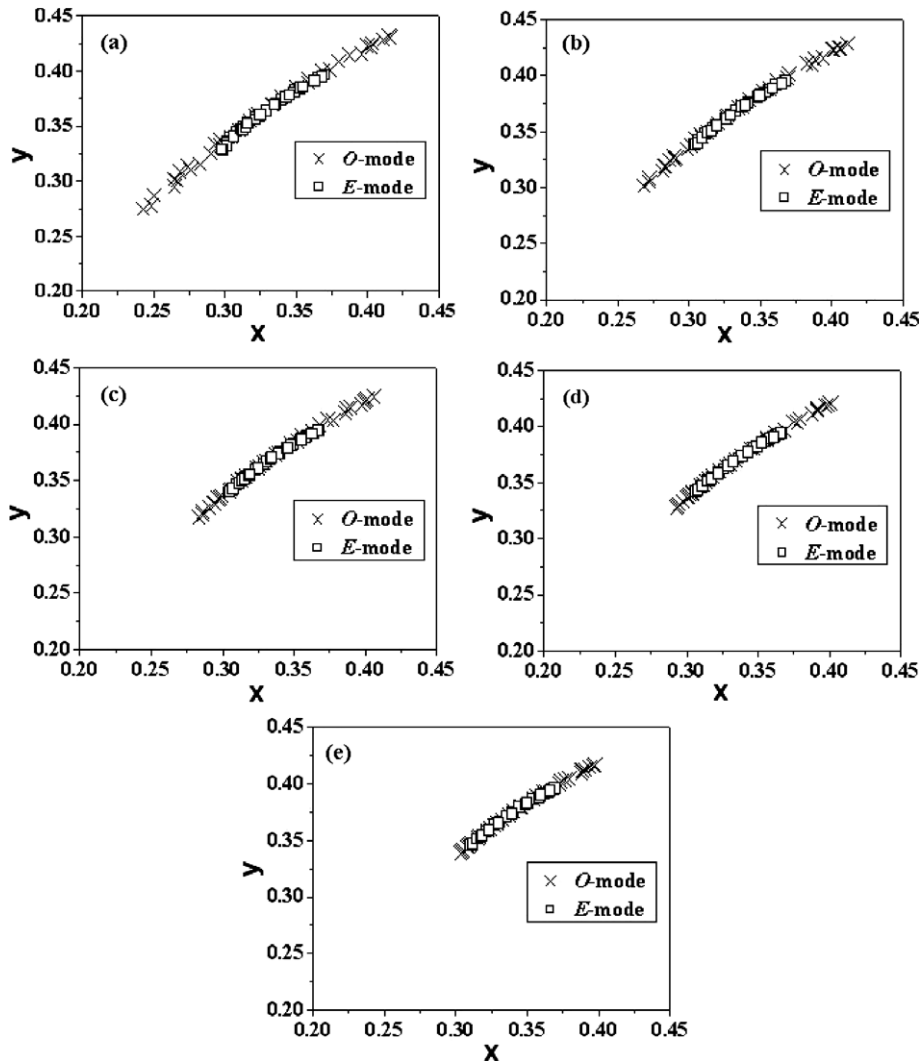


Fig. 4. Calculated color shift characteristics at (a) T_{20} , (b) T_{40} , (c) T_{60} , (d) T_{80} , and (e) T_{100} with E- and O-modes.

results and this implies that the dark states are the same as one another in both cases.

In terms of the viewing angle considering both luminance uniformity and contrast ratio, neither mode shows distinct differences. However, the shift of color chromaticity depending on the viewing angle shows a clear difference between the two modes. Fig. 4 shows the shift of color chromaticity (x, y) [14] according to the viewing directions in several grey levels such as T_{20} , T_{40} , T_{60} , T_{80} , and T_{100} . Here, the results are obtained at a polar angle of 60° by changing the azimuthal angle from 0° to 360° with a step of 10° . As clearly presented in Fig. 4, the device with the E-mode shows much less color shift than that in an O-mode, although as the grey level approaches white state, the difference between them is reduced. To understand in detail how the x and y color coordinates change according to the viewing direction, we observed color coordinates of the white state at a fixed polar angle of 60° along all azimuthal directions, as shown in Fig. 5. Since the LC director is aligned 12° in an azimuthal angle and in white state it is rotated about 45° on average, both color coordinates oscillate with troughs at 57° and 237° and crests at 147° and 327° , which are approximately coincident with directions parallel and perpendicular to the LC director exhibiting bluish and yellowish color shift in white state, respectively [5]. However, the degree of variation of the color coordi-

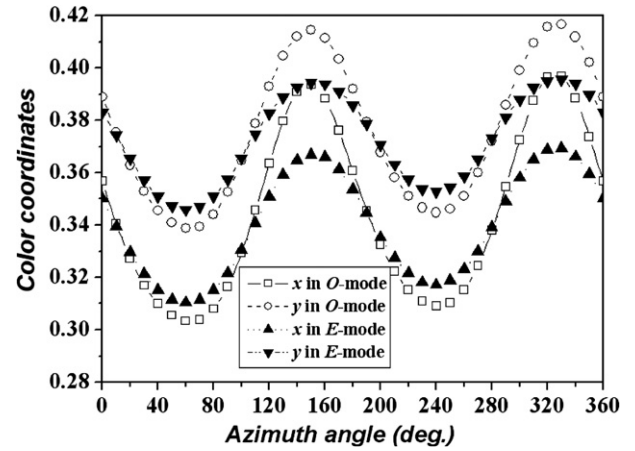


Fig. 5. Variation of color coordinates in T_{100} at 60° polar angle along azimuthal direction with the O- and E-modes.

nates along azimuthal directions is much higher in the O-mode than in the E-mode, indicating that the device with the O-mode in oblique viewing direction shows more bluish and yellowish color shift at specific directions than that with the E-mode. To compare the color shift of several greys in two specific azimuthal directions of 147° and 237° , wavelength dispersion of the transmitted light is calculated at a polar angle of 60° . As mentioned above, the

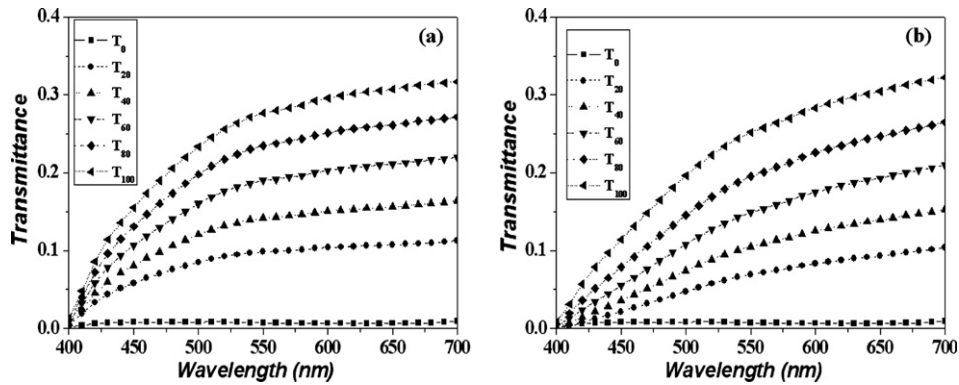


Fig. 6. Wavelength dispersion at 60° polar angle in (a) E- and (b) O-modes when an azimuthal direction is 135° .

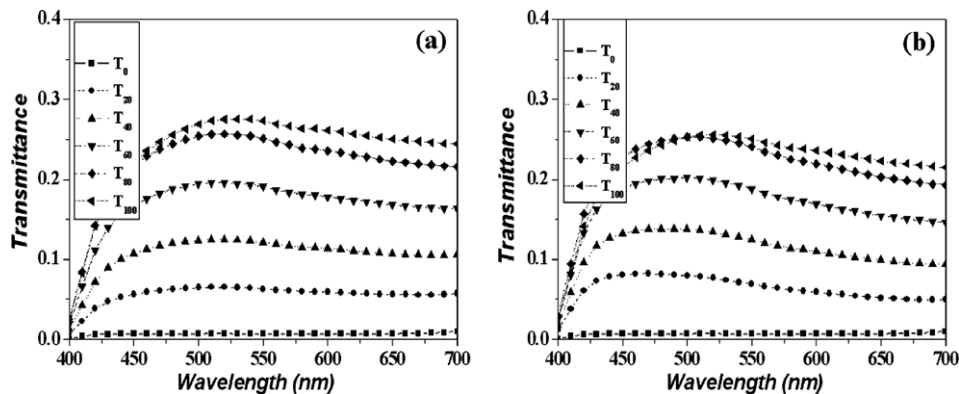


Fig. 7. Wavelength dispersion at 60° polar angle in (a) E- and (b) O-modes when the azimuthal direction is 225° .

yellowish color shift occurs at an azimuthal angle of 147°, that is, blue light is transmitted much less than red light, as shown in Fig. 6. It should be noted that transmitted blue light is much more suppressed in the O-mode than in the E-mode. Relatively, the difference between the two modes at an azimuthal angle of 237° is not so large but the device with O-mode shows slightly more wavelength dispersion than that with E-mode, such that the peak wavelength

exists at a relatively shorter wavelength in the O-mode than in the E-mode, indicating that the O-mode shows more bluish color than the E-mode, as shown in Fig. 7.

Previous work also reported that the color chromaticity of the 90° twisted nematic (TN) LC mode was strongly dependent on the O- and E-modes [15]. Now the question arises why the FFS mode where molecular orientation changes periodically along electrode positions should

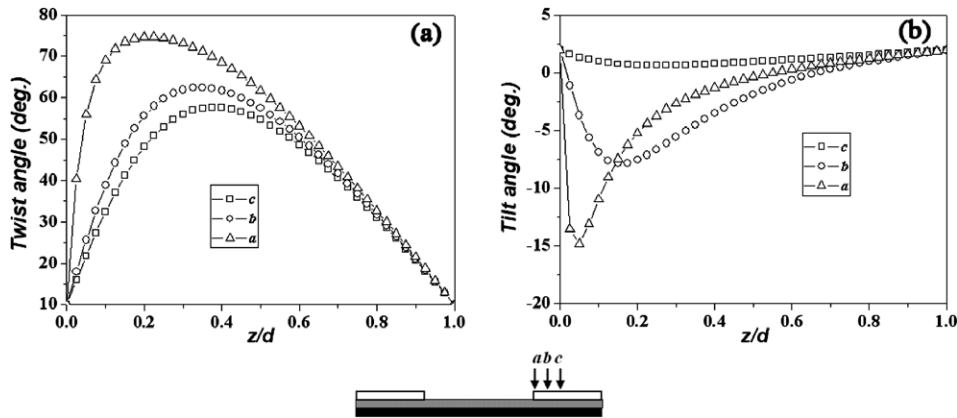


Fig. 8. Director profile of (a) twist and (b) tilt angles at three different electrode positions.

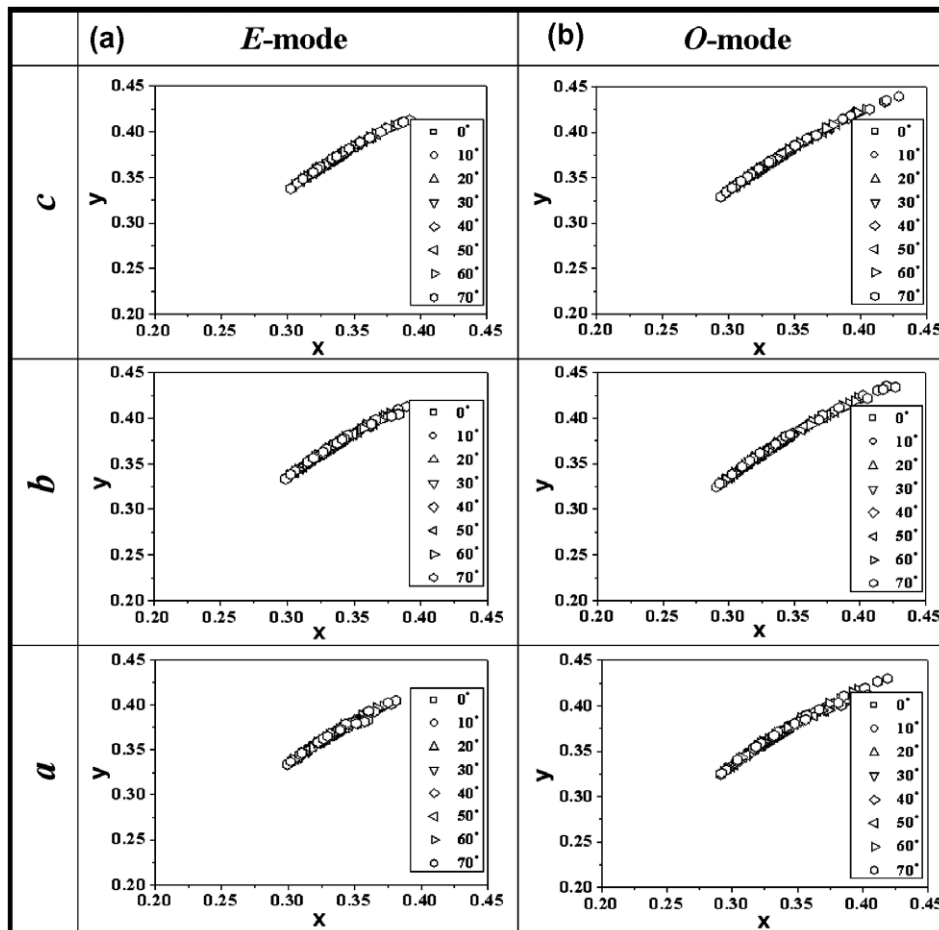


Fig. 9. Color shift at three different electrode positions depending on (a) E- and (b) O-modes.

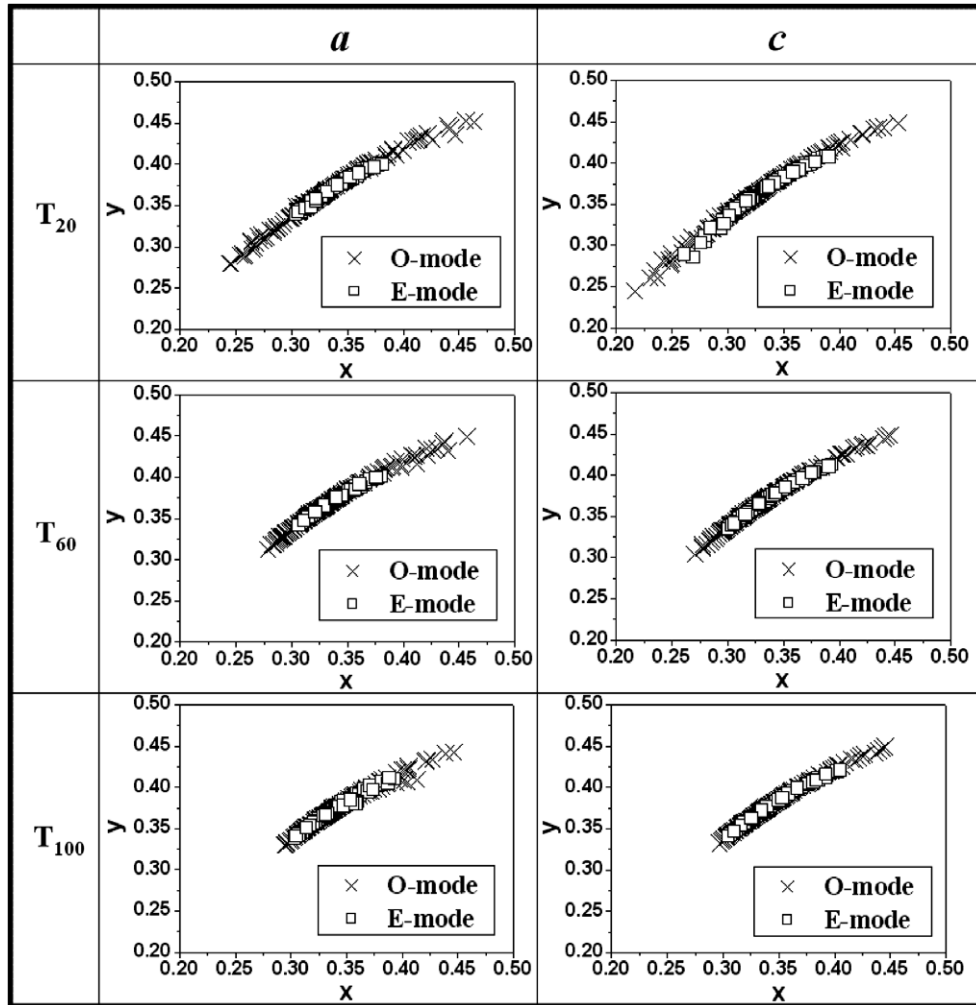


Fig. 10. Color shift at two electrode positions *a* and *c* depending on E- and O-modes in several grey levels.

exhibit such a phenomenon. In order to understand this, we calculated molecular orientation in the white state at three positions: edge (*a*), center (*c*), and between center and edge (*b*) of the pixel electrode since the LC orientations in those positions comprise a repeated basic unit so that they can represent the behavior of the device well [16], as shown in Fig. 8. At the edge of electrodes, the maximal twist angle of 63° from initial orientation occurs near the bottom substrate, that is, $z/d = 0.2$ and it decreases rapidly as the vertical distance approaches the top substrate. However, at positions *b* and *c*, the maximal twist angles occur at $z/d = 0.35$ and 0.37 with twist angles of 52° and 47°, respectively. Since the tilt angles in the white state are not as large, we know that the LC orientation at position *a* is similar to that in a 63° twisted TN and at position *c* it is quite similar to the LC orientation in the IPS mode. This indicates that at position *c*, the optic axis in white state exists so that the light modulation occurs by phase retardation, while at position *a*, the optic axis in white state does not exist, so that the light modulation is related to the polarization rotation effect. With information on the LC orientations along electrodes, the degree of color shift is

calculated at each electrode position up to 70° of polar angle in all azimuthal directions. As presented in Fig. 9,

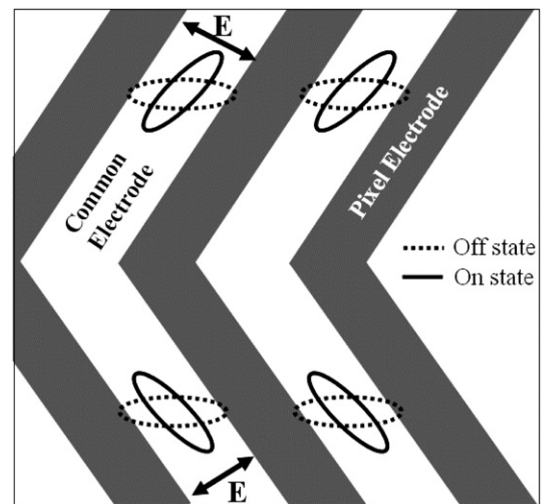


Fig. 11. Schematic top view of a cell structure showing that the LC director rotates in two opposite directions due to two different field directions in a pixel.

the degree of color shift (Δxy) is much higher in the O-mode than in the E-mode at all electrode positions, such that the Δxy values are 0.108 and 0.117 for E-mode, and 0.166 and 0.175 for the O-mode at positions a and c , respectively. Nevertheless, the LC orientation at electrode position a shows the least color shift, irrespective of modes. In the previous description, we claimed that the difference in color shift between modes becomes reduced with increasing grey levels (see Fig. 4). To understand the origin of this behavior, we calculate color shift depending on modes at two electrode positions a and c in several grey levels, as shown in Fig. 10. At electrode position a , the Δxy increases slightly from 0.098 at T_{20} to 0.115 at T_{100} in the E-mode, while it decreases strongly from 0.278 at T_{20} to 0.186 at T_{100} in the O-mode. Consequently, the color difference Δ between the two modes defined as $\Delta = |\Delta xy_{E\text{-mode}} - \Delta xy_{O\text{-mode}}|$ at electrode position a decreases from 0.18 at T_{20} to 0.07 at T_{100} . At electrode position c , the Δxy decreases from 0.175 at T_{20} to 0.128 at T_{100} in the E-mode, while it decreases strongly from 0.312 at T_{20} to 0.189 at T_{100} in the O-mode. As a result, the color difference Δ between the two modes at electrode position c decreases from 0.137 at T_{20} to 0.061 at T_{100} . These results clearly show that the difference between two modes is much higher at low grey level than at high grey level and it decreases rapidly as the grey level approaches a white state at all electrode positions. However, the color shift in region c , at which the light modulation occurs by the phase retardation effect, has stronger dependence on the initial cell configuration than that in region a , at which the light modulation

occurs by the polarization retardation effect. In other words, wavelength dispersion of Δn_{eff} at position c is much higher than at position a . Consequently, the FFS device with the E-mode is advantageous to achieve a high image quality for a single domain device in which the LC director rotates in one direction.

In the case of a large-sized FFS mode, a wedge electrode is used to imitate a dual domain LC configuration [17], as shown in Fig. 11. Here, the common electrode exists as a plane and above it the pixel electrode exists as a wedge, with passivation layer between them. In this way, the field direction in one half of a pixel is different from that in the other half, so that the LC director in the top half rotates anticlockwise, while that in the bottom half rotates clockwise. As a result, the degree of color shift is reduced due to a self-compensation effect. The degree of color shift depending on the E- and O-modes is calculated in this dual domain structure at several grey levels T_{20} , T_{40} , T_{60} , and T_{80} , as shown in Fig. 12. The difference between the two modes at all grey levels is greatly reduced and further, the degree of color shift is greatly reduced as the grey level approaches a white state. However, the E-mode still shows less color shift than the O-mode. The good-suppression of color shift at a white state is attributed to the perfect self-compensation effect, such that the LC director in one half of a pixel is perpendicular to that in the other half of a pixel on average.

To confirm the calculated results, we fabricated unit cells in which the cell conditions are similar to those in the calculation and measured the color shift for the

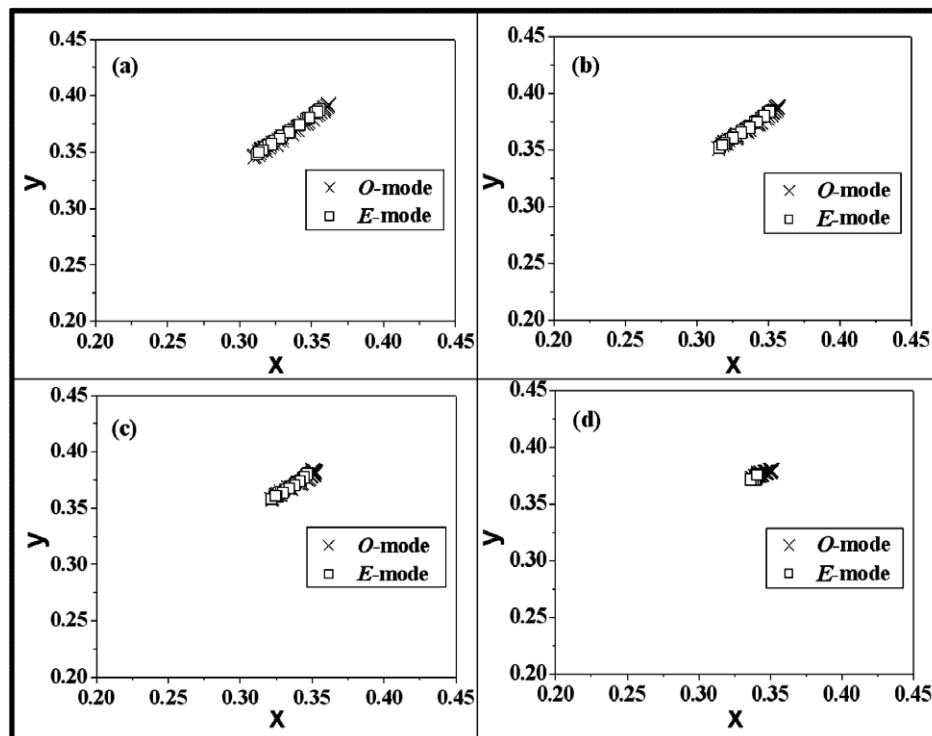


Fig. 12. Calculated color characteristics at (a) T_{40} , (b) T_{60} , (c) T_{80} and (d) T_{100} with O- and E-modes in a dual domain FFS mode.

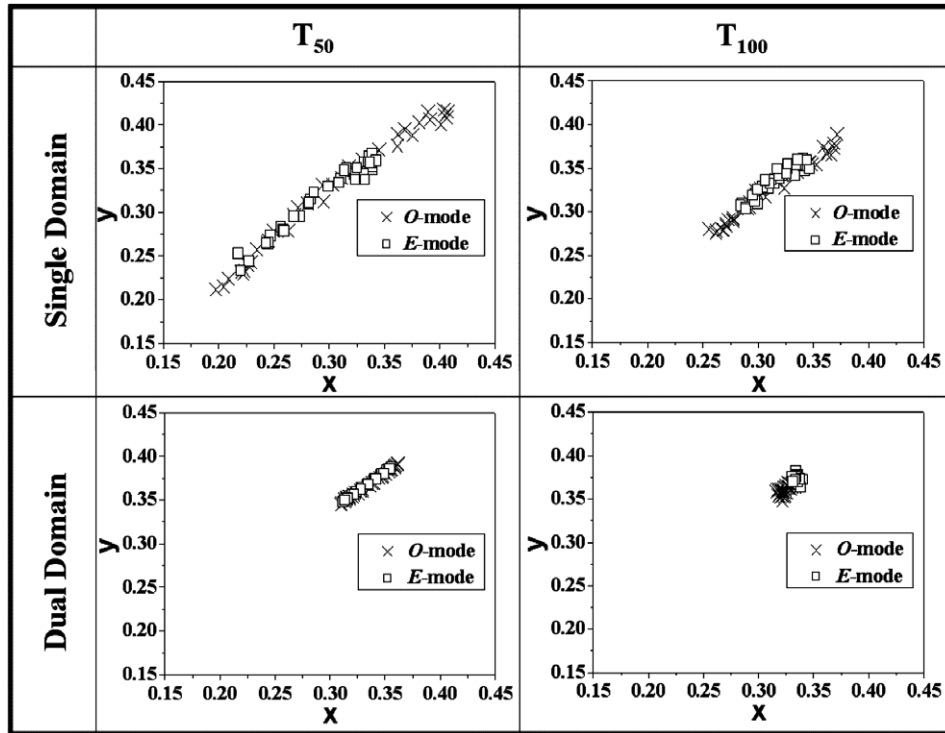


Fig. 13. Measured color characteristics at T_{50} and T_{100} with O- and E-modes in single and dual domain FFS modes.

E- and O-modes at two grey levels T_{50} and T_{100} , as shown in Fig. 13. As clearly indicated, the degree of color shift is much stronger at low grey level than at high grey level and further the degree of color shift in a single domain is much stronger than that in the dual domain. The difference in color shift between two modes is stronger in the single domain than in the dual domain at all grey levels. However, in the dual domain cell, the difference between two modes is greatly reduced.

4. Conclusions

We have studied the degree of color shift depending on the E- and O-modes in the fringe-field switching mode using a LC with negative dielectric anisotropy. All electrode positions that have LC orientation similar to low TN and IPS devices show strong dependence of color shift on modes. This dependency slightly decreases as the grey level approaches a white state. Conclusively speaking, in a single domain FFS mode, the FFS device with E-mode is more advantageous to reduce the color shift according to the viewing direction; however, the difference is much more highly suppressed in a dual domain structure.

Acknowledgement

This research was supported by a grant (F0004132) from the Information Display R&D Center, one of the 21st Century Frontier R&D Programs funded by the Ministry of

Commerce, Industry and Energy of the Korean Government.

References

- [1] M. Oh-E, K. Kondo, *Jpn. J. Appl. Phys.* 36 (1997) 6798.
- [2] S.H. Lee, S.L. Lee, H.Y. Kim, *Asia Display '98* (1998) 371.
- [3] S.H. Lee, S.L. Lee, H.Y. Kim, *Appl. Phys. Lett.* 57 (1998) 2881.
- [4] S.H. Hong, I.C. Park, H.Y. Kim, S.H. Lee, *Jpn. J. Appl. Phys.* 39 (2000) 527.
- [5] H.Y. Kim, G.R. Jeon, D.-S. Seo, M.-H. Lee, S.H. Lee, *Jpn. J. Appl. Phys.* 41 (2002) 2944.
- [6] S.H. Lee, H.Y. Kim, S.M. Lee, S.H. Hong, J.M. Kim, J.W. Koh, J.Y. Lee, H.S. Park, *SID 01 Digest* (2001) 117.
- [7] A. Takeda, S. Kataoka, T. Sasaki, H. Chida, H. Tsuda, K. Ohmuro, Y. Koike, T. Sasabayashi, K. Okamoto, *SID 98 Digest* (1998) 1077.
- [8] Y. Saitoh, S. Kimura, K. Kusafuka, H. Shimizu, *Jpn. J. Appl. Phys.* 37 (1998) 4822.
- [9] J.E. Anderson, P.J. Bos, *Jpn. J. Appl. Phys.* 39 (2000) 6388.
- [10] I.S. Song, H.K. Won, D.S. Kim, H.-S. Soh, W.Y. Kim, S.H. Lee, *Jpn. J. Appl. Phys.* 43 (2004) 4242.
- [11] S.H. Hong, H.Y. Kim, J.-H. Kim, S.-H. Nam, M.-H. Lee, S.H. Lee, *Jpn. J. Appl. Phys.* 41 (2002) 4571.
- [12] S.H. Jung, H.Y. Kim, M.-H. Lee, J.M. Rhee, S.H. Lee, *Liq. Cryst.* 32 (2005) 267.
- [13] A. Lien, *Appl. Phys. Lett.* 57 (1990) 2767.
- [14] B. Bahadur, *Liquid Crystals – Applications and Uses*, Vol. 2, World Scientific, Singapore, 1991 (Chapter 8).
- [15] H. Takano, S. Suzuki, H. Hatoh, *IBM J. Res. Develop.* 36 (1992) 23.
- [16] H.Y. Kim, S.H. Hong, J.M. Rhee, S.H. Lee, *Liq. Cryst.* 30 (2003) 1285.
- [17] S.H. Lee, S.M. Lee, H.Y. Kim, J.M. Kim, S.H. Hong, Y.H. Jeong, C.H. Park, Y.J. Choi, J.Y. Lee, J.W. Koh, H.S. Park, *SID 01 Digest* (2001) 484.